Int. J. Heat Mass Transfer. Vol. 15, pp. 769–780. Pergamon Press 1972. Printed in Great Britain

EFFECT OF FREE-STREAM TURBULENCE ON MASS TRANSFER FROM A CIRCULAR CYLINDER IN CROSS FLOW

TOKURO MIZUSHINA, HIROMASA UEDA and NOBUYUKI UMEMIYA
Department of Chemical Engineering, Kyoto University, Kyoto, Japan

(*Received* 30 *September* 1970)

Abstract—Overall and local mass transfer at large Schmidt number range from a circular cylinder in cross flow are presented. Measurements of the mass transfer were made by means of electrochemical method at three levels of the turbulence intensity, i.e. $Tu = 0{\cdot}8$, $1{\cdot}2$ and $2{\cdot}3$ per cent, and Reynolds number range from 3870 to 10380.

The effect of the screen-produced turbulence in the free stream on the overall and the local mass-transfer rates was determined at large Schmidt number of 1230. In addition, the effect of the turbulence on the location of the separation point was determined.

NOMENCLATURE

A, surface area of mass transfer [cm^2];
$a_1, \ldots a_7$, coefficients in equation (16);
c, concentration [g mole/cm^3];
c_f, friction factor $= \tau_w/\frac{1}{2}\rho U_\infty^2$;
c_p, pressure coefficient defined by equation (15);
D, diameter of cylinder [cm];
$\mathscr{D}$, molecular diffusivity [cm^2/s];
E_0, E_1, coefficients in equation (10);
F, Faraday constant [As/g-equivalent];
i, electric current [A];
j_D, j factor of mass transfer;
j_H, j factor of heat transfer;
k, mass-transfer coefficient [cm/s];
N, mass-transfer rate [g mole/cm^{2}s];
Nu, Nusselt number;
n_e, valence charge of an ion;
p, pressure [g/cm s^2];
Pr, Prandtl number;
R, radius of cylinder [cm];
Re, Reynolds number;
Sc, Schmidt number;
Sh, Sherwood number;
Sh_0, Sherwood number at zero turbulence intensity;
Tu, turbulence intensity $= 100\sqrt{(\bar{u}'^2)}/U_\infty$;
u, velocity in x direction [cm/s];
$U(x)$, velocity at outer edge of boundary layer [cm/s];
U_∞, free stream velocity [cm/s];
v, velocity in y direction [cm/s];
W, duct width [cm];
x, distance from front stagnation point along the circumference of cylinder [cm];
y, distance from surface of cylinder [cm].

Greek symbols

α, coefficient of equation (3) [A];
β, coefficient of equation (3) [A s$^{\frac{1}{2}}$/cm$^{\frac{1}{2}}$];
η, coordinate defined by equation (9);

θ, angle from front stagnation point [degree];
Λ, wedge variable defined by equation (11);
μ, viscosity [g/cms];
ν, kinematic viscosity [cm^2/s];
ξ, coordinate defined by equation (8);
ρ, density [g/cm^3];
τ_w, skin friction [g/cms^2];
ϕ, frequency [1/s].

Subscripts

b, bulk;
s, front stagnation point;
sep, separation point;
x, local value at x;
w, wall;
∞, free stream.

INTRODUCTION

IT HAS been known for a long time that the heat transfer from a body in cross flow is increased when the free-stream turbulence intensity is increased, and recently many experimental results concerning this effect have been reported, particularly for the overall coefficients of heat transfer from a circular cylinder in an air stream.

The first quantitative investigation was carried out by Comings *et al.* [1], who measured the influence of turbulence on the overall heat transfer in the subcritical Reynolds number range from 400 to 20000. They found that if the Reynolds number was high enough, the overall heat transfer coefficient increased with the turbulence intensity in the lower turbulence intensity region, tending toward a definite value at higher turbulence intensities, but the effect was negligible at smaller Reynolds numbers. The effects of turbulence are divided into an increase in local heat-transfer rate, an earlier transition to turbulent boundary layer, a movement of the separation point, and a change of flow mechanism in the separated region. Giedt [2] measured the local skin friction and local rate of heat transfer in the ranges of near-critical and super-critical Reynolds number, and found the very important fact that the distribution of the skin friction coefficient around the front portion of the cylinder remained virtually unaffected by a considerable increase in free-stream turbulence intensity. Kestin and Maeder [3] made an extensive discussion of this problem and reported experimental results of the effect of screen-produced turbulence on the overall coefficient of heat transfer from a cylinder in an air stream in the near-critical Reynolds number range. These results demonstrate that the heat-transfer rate is increased substantially by a slight increase in the turbulence intensity, and that it becomes almost constant with further increases in the turbulence intensity.

In spite of the existence of many experiments on the overall heat transfer in cross flow, there have been few investigations on the effect of turbulence on the local values of heat or mass transfer from circular cylinders in cross flow, especially for high Prandtl or Schmidt numbers.

The purpose of this paper is the presentation of the effects of screen-produced turbulence on the local mass-transfer rate at high Schmidt numbers. The measurements were made in subcritical Reynolds number range from 3870 to 10380 and at free-stream turbulence of 0·8, 1·2 and 2·3 per cent. The investigation of such a moderate Reynolds number region is quite necessary, since in most cases in chemical industries, the operations of heat and mass transfer in liquid flow are carried out in this Reynolds number range. However, such investigations have been very few, even for the overall heat transfer, in contrast to the many investigations in the near-critical Reynolds number range.

In the present investigation, the electrochemical method [4] is used to measure the rates of mass transfer around a cylinder perpendicular to the liquid flow. This method is based on a diffusion-controlled electrode reaction, and is convenient for the measurement of the local mass-transfer rate, which is detected by an

electric current on a small electrode isolated from surrounding mass-transferring electrode surface.

Pressure distributions were measured at Reynolds numbers $Re = 10300$ and 7320. These results enable us to make theoretical predictions of the local mass-transfer rate. Since the local mass-transfer rates predicted from pressure distribution may be regarded as the values for zero turbulence intensity, they will be used as the bases for estimating the effects of turbulence on the local mass-transfer rate.

EXPERIMENTAL METHOD

The electrochemical method is based on a diffusion-controlled electrode reaction. In this experiment, the redox system of ferricyanide and ferrocyanide ion was used:

$$Fe(CN)_6^{3-} + e^- \rightarrow Fe(CN)_6^{4-}. \qquad (1)$$

The reaction occurs at the surface of the test electrode, i.e. mass-transfer surface in the presence of a large excess of sodium hydroxide which eliminates the migration of ferricyanide ions in the electric field.

In such a condition, the transport of the ions is controlled only by diffusion and convection. The reaction at the surface of the electrode proceeds at such a rapid rate that the concentration at the surface of the test electrode is constant and essentially equal to zero. Thus, the transport of the ions is treated as ordinary mass-transfer problem or simulated as heat transfer with constant wall temperature. The total rate of mass transfer to the electrode may be written as

$$N = \frac{i}{An_eF} = k(c_b - c_w) = kc_b. \qquad (2)$$

Making use of this equation, one obtains the mass-transfer coefficient k from the measurement of the electric current i. In the present investigation this method is also employed to measure the free stream turbulence intensity. The liquid velocity is related to the electric current on the small electrode of the velocity measuring probe. The relation is analogous to that of a hot wire anemometer, and is expressed as

$$i = \alpha + \beta u^{0.5}. \qquad (3)$$

Its response to high frequency velocity fluctuation is influenced only by the capacitance effect of the concentration boundary layer. A calculation of the response showed that the critical frequency at which the amplitude ratio goes down to 0·9 when the velocity measuring probes are placed in a stream of velocity $u = 100$ cm/s is given as follows;

Sc = 1230 wire ($d = 0{\cdot}0010$ cm):
$\phi_{crit} = 6430$ Hz, phase lag = 24·9 degree
sphere ($d = 0{\cdot}0010$ cm):
$\phi_{crit} = 8120$ Hz, phase lag = 27·0 degree

The critical frequency is so large that this method needs no compensation for phase shift and amplitude decrease. A detailed description of the electrochemical method is given in [4].

EXPERIMENTAL APPARATUS AND PROCEDURE

The experimental apparatus is shown schematically in Fig. 1. A test cylinder of 1 cm dia. was mounted horizontally in a channel of 8 × 16 cm cross section, its axis being perpendicular to the free stream. The flow system, i.e. the water tunnel and pump were made of polyvinylchloride plastic. Two types of test cylinder having diameter of 1 cm were used: the one for pressure distribution measurements having a static pressure tap of 0·5 mm dia., and the one for mass-transfer measurements having platinum cathode of 0·5 mm dia., which is imbedded in, but isolated electrically from the main cathode covering around the middle part of the cylinder surface in width of 2 cm. Both the isolated cathode and the main cathode were active during the measurements. The anode, which was a large nickel plate of 20 × 10 cm, was located downstream. The cylinders can be rotated during the experiments, so as to make the position of the pressure tap or the isolated

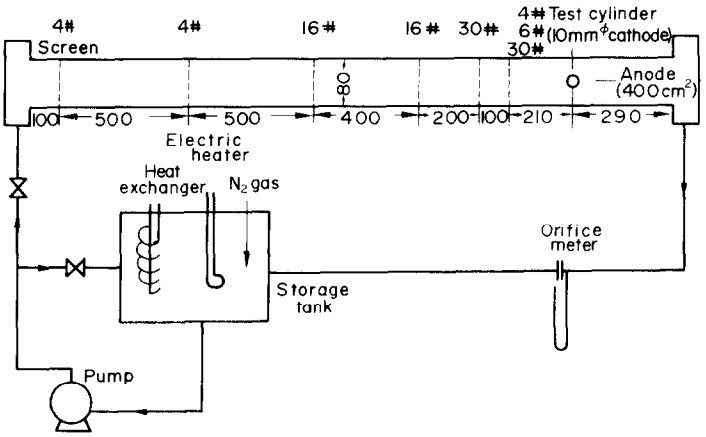

FIG. 1. Schematic diagram of the experimental apparatus.

cathode relative to the front stagnation point vary.

The circulating solution contained 0·01 mole of $K_3Fe(CN)_6$ and $K_4Fe(CN)_6$ respectively, and 1 mole of NaOH per litre, and was kept at 30°C. The oxygen in the solution was purged with nitrogen before each experimental run. To make the velocity profile as flat as possible, five screens were installed in series in the channel upstream from the test cylinder. The turbulence intensities were changed from 0·8 to 2·3 per cent by changing the screens located 21 cm upstream from the test cylinder.

EXPERIMENTAL RESULTS AND DISCUSSION

(a) *Overall mass-transfer coefficient*

In Fig. 2, the results of overall mass-transfer coefficient are plotted in the form of j-factor as a function of Reynolds number. Reynolds number is based on the free-stream velocity corrected for solid-blocking and for wake-blocking after Pope's method [5], which gives 1·029 as the correction factor for the free stream velocity. The results obtained by other investigators are also plotted in Fig. 2. Among those, Grassmann's data [6] were obtained from the mass-transfer measurements by the electrochemical method. As pointed out by Comings *et al.*, the effect of turbulence appears at high Reynolds numbers in this investigation. In this study the overall mass-transfer coefficients were obtained with three levels of free-stream turbulence intensity, i.e. 0·8, 1·2 and 2·3 per cent.

The data for turbulence intensities of 1·2 and 2·3 per cent are in good agreement with the heat-transfer results by Comings *et al.* and the mass-transfer ones by Grassmann *et al.* corrected for blocking effects, and the data for the turbulence intensity of 0·8 per cent agree with Hilpert's heat-transfer data [7] for the intensity = 0·3 per cent. The effect of turbulence was studied by Kestin and Maeder [3] in heat transfer from a cylinder in air stream. Their results together with the authors' results are shown in Fig. 3. Agreement between the results for $Pr = 0{\cdot}7$ and those for $Sc = 1230$ is good. Therefore, the analogy between heat and mass transfer is confirmed even in the effect of turbulence.

(b) *Local mass-transfer coefficients*

(1) *Theoretical predictions of the local mass-transfer coefficients for zero turbulence intensity from the measurements of static pressure distribution.* To estimate the effect of turbulence on the local mass-transfer rate, the local values of the

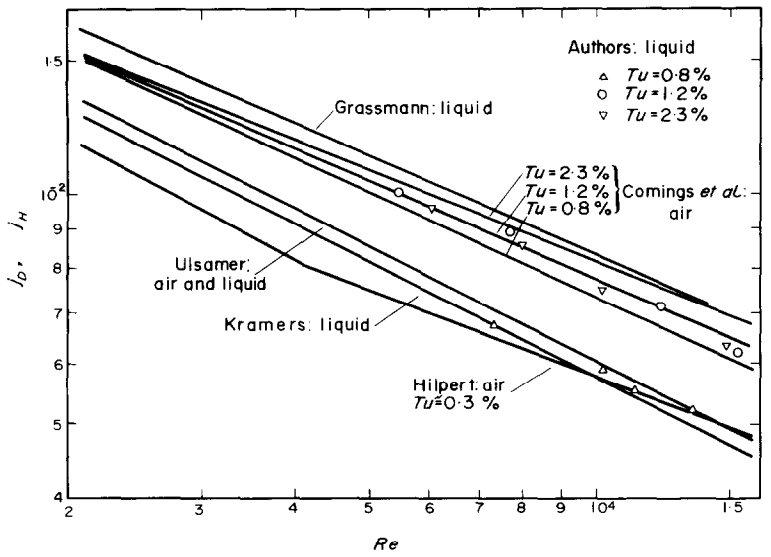

FIG. 2. Overall heat and mass-transfer rate around a cylinder in cross flow.

mass-transfer coefficient for zero turbulence intensity are necessary as the basic values. However, these values may not be obtained experimentally since the wake of the cylinder increases the turbulence in the approaching flow, even in a low-turbulence wind tunnel. Hence theoretically predicted values will be regarded as the basic values. Hereafter, the discussion will be limited only to the laminar boundary layer at the front portion of the cylinder, up to the separation point.

Since the diffusion of momentum and mass occurs in a thin layer on the wall in this region, the usual boundary layer assumptions are

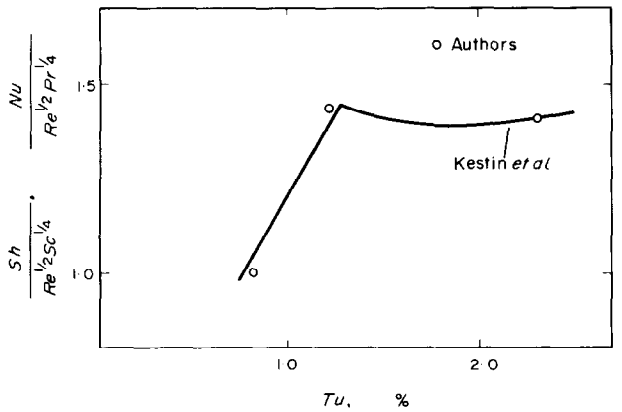

FIG. 3. Effect of turbulence on the overall mass-transfer coefficient.

valid and the governing differential equations and boundary conditions are the same as those of heat transfer to a geometrically similar surface with constant wall temperature.

Equation of motion:

$$u\frac{\partial u}{\partial x}+v\frac{\partial u}{\partial y}=U\frac{\mathrm{d}U}{\mathrm{d}x}+\nu\frac{\partial^2 u}{\partial y^2}. \tag{4}$$

Equation of continuity:

$$\frac{\partial u}{\partial x}+\frac{\partial v}{\partial y}=0. \tag{5}$$

Conservation of mass:

$$u\frac{\partial c}{\partial x}+v\frac{\partial c}{\partial y}=\mathscr{D}\frac{\partial^2 c}{\partial y^2}. \tag{6}$$

Boundary conditions:

$$u(x,y)=v(x,y)=0,\quad c(x,y)=c_w=0 \text{ at } y\to 0$$
$$u(x,y)=U(x),\quad c(x,y)=c_b \text{ at } y\to\infty. \tag{7}$$

where x is the distance from the front stagnation point along the circumference of the cylinder, and y is the distance from the surface. The external velocity, i.e. the velocity at the outer edge of the boundary layer, $U(x)$, is presumed to be determined from pressure distribution. N. Froessling [8] obtained an exact solution of this problem by using a power series, and presented a table of its coefficients for the case of $Pr=0{\cdot}7$. Since these coefficients depend on the Prandtl number, further numerical evaluation is needed for high Prandtl or Schmidt numbers. Therefore, in this study, the following three methods have been used.

The first, due to W. Dienemann [9], is a simple extension of Pohlhausen's method for velocity boundary layer and based on equations which are the integral form of equations (4) and (6) and on the polynomial temperature distribution to the fourth degree.

The second, due to H. J. Merk [10] is an extension of Meksyn's method [11] for velocity boundary layer, and uses the "wedge solution", i.e. the solution of the boundary-layer equation for the flow past a wedge. This method consists of transformation of variables of equations (4) and (6), that is

$$\xi=\int_0^x\frac{U(x)}{U_\infty}\frac{\mathrm{d}x}{R} \tag{8}$$

$$\eta=\left(\frac{Re}{2\xi}\right)^{\frac{1}{2}}\frac{U(x)}{U_\infty}\frac{y}{R}. \tag{9}$$

The solutions of the transformed equations are determined in the form of a series expansion. The local Sherwood number is

$$Sh=\frac{U(x)/U_\infty}{2\times 2\xi}\left(E_0+2\xi\frac{\mathrm{d}\Lambda}{\mathrm{d}\xi}E_1+\ldots\right)\sqrt{Re} \tag{10}$$

where the quantities E_0 and E_1 are functions of the Schmidt number and the "wedge variable" defined as

$$\Lambda=\frac{2\xi}{[U(x)/U_\infty]^2}\frac{\mathrm{d}[U(x)/U_\infty]}{\mathrm{d}(x/R)}. \tag{11}$$

The terms beyond the first in equation (10) are relatively small if ξ and, or $\mathrm{d}\lambda/\mathrm{d}\xi$ are small, and may be neglected. The estimation of the error by neglecting them has not been done, but the solution is in good agreement with the exact solution in the case of $Pr=0{\cdot}7$. Therefore, this method seems to give satisfactory prediction even for high Schmidt numbers.

As the third method, the Lévêque's solution [12] is employed. This is an exact solution when a concentration boundary layer is so thin that the velocity profile may be assumed to be linear. In the case of high Schmidt numbers, this assumption may be valid. The velocity gradient at the wall may be calculated exactly with Blasius series by using the measured pressure distribution.

At the front stagnation point, the exact solution for the mass-transfer coefficient may be obtained from the following equations:

$$Sh=\alpha(Sc)\,(u_1 d^2/\nu)^{\frac{1}{2}} \tag{12}$$

$$\frac{1}{\alpha(Sc)}=\int_0^\infty\exp\left[-Sc\int_0^\eta f(\eta)\,\mathrm{d}\eta\right]\mathrm{d}\eta \tag{13}$$

where u_1 is $dU(x)/dx$ at the front stagnation point, and the function $f(\eta)$ represents the velocity distribution in the boundary layer. Equations (12) and (13) were derived by Squire [13] and were used in the present study for high Schmidt numbers by evaluating numerically $\alpha(Sc)$ from tabulated values [14] for $f(\eta)$.

$$c_p = \frac{p - p_\infty}{\frac{1}{2}\rho U_\infty^2}. \tag{15}$$

Since the laminar region is of particular interest with regard to the boundary layer prediction, the calculated values of $U(x)/U_\infty$ for the front portion of the cylinder up to the separation

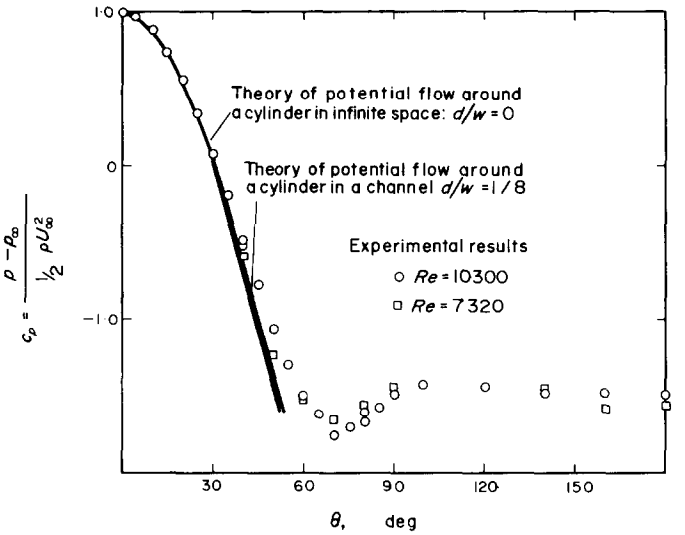

FIG. 4. Distribution of static pressure around a cylinder in cross flow.

(2) *Distributions of static pressure,* $U(x)/U_\infty$ *and local friction factor.* For the prediction of the velocity and concentration gradients in the boundary layers, the distribution of static pressure needs to be measured. The measured pressure distribution is plotted in Fig. 4 together with the predictions of the potential flow theories.

The velocity distribution at the outer edge of the boundary layer is determined after Bernoulli's theorem:

$$U(x)/U_\infty = (1 - c_p)^{\frac{1}{2}} \tag{14}$$

where c_p is the pressure coefficient, which is defined by the following equation.

point are plotted in Fig. 5 together with the results obtained by Hiemenz [15] at Reynolds number $Re = 18400$. The distributions predicted from the potential flow theory are also plotted. In spite of the difference of the Reynolds numbers, the velocity distributions calculated from the measured pressure distribution agree very well with each other, especially near the stagnation point. This fact has been examined in detail by Giedt and Sogin [16]. They also found an important fact that the pressure distribution near the stagnation point remained virtually unaffected by an increase of turbulence. These facts permit us to use the measured pressure distribution at any values of Reynolds number

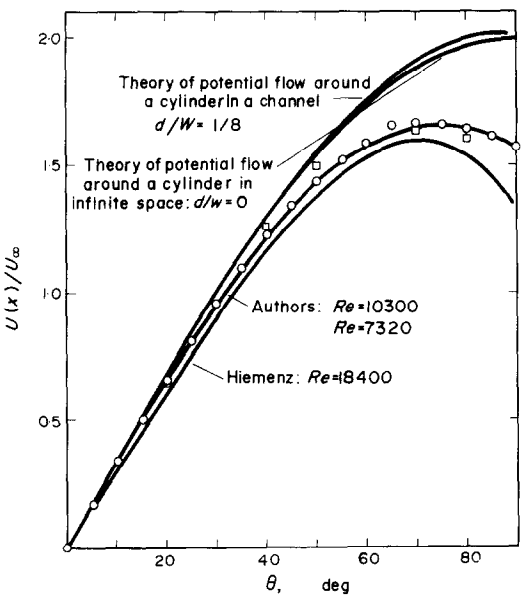

FIG. 5. Distribution of $U(x)/U_\infty$ calculated from measurements of the static pressure distribution.

and turbulent intensity for the prediction of mass transfer at zero turbulence intensity. The equation correlating the plots in Fig. 5 is obtained by the least square method as in the form:

$$\frac{U(x)}{U_\infty} = a_1\left(\frac{x}{R}\right) + a_3\left(\frac{x}{R}\right)^3 + a_5\left(\frac{x}{R}\right)^5 + a_7\left(\frac{x}{R}\right)^7. \qquad (16)$$

Table 1 shows the determined values of the coefficients in equation (16), and also includes the ones by Hiemenz and by Schmidt and Wenner.

Using equation (16), one can calculate the local skin friction by Pohlhausen's approximate method, by Meksyn's approximate method and by the Blasius series respectively. As seen in Fig. 6, these three results agree very closely with each other near the stagnation point, and diverge as the angular coordinate θ increases because all of these methods become inaccurate near the separation point. Since the separation point is the point where the local skin friction is zero, it is determined from Fig. 6 to be at $\theta_{sep} = 87{\cdot}6^\circ$, $78{\cdot}7^\circ$ and $85{\cdot}2^\circ$ by the first, second and third methods respectively, though the accuracy is questionable.

(3) *Distributions of local mass-transfer coefficient.* In Fig. 7 the predicted values of the local mass-transfer coefficient obtained by the three approximate methods described in the

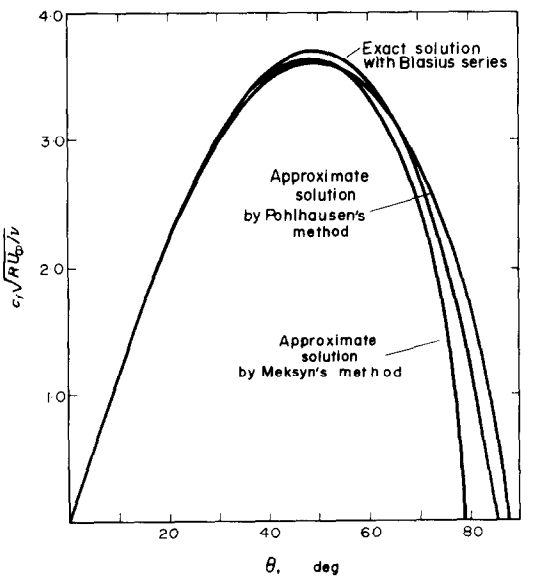

FIG. 6. Local skin friction around the cylinder in cross flow, calculated from distribution of $U(x)/U_\infty$.

Table 1. *Coefficients* a_1, a_3, a_5 *and* a_7 *in equation* (16)

Re	a_1	a_3	a_5	a_7	Investigators
10300	1·9776	−0·50597	0·084088	−0·016946	Authors
7320	1·9707	−0·45327	0·023894		Authors
18400	1·8157	−0·2714	−0·047325		Hiemenz [15]
170000	1·8155	−0·4094	−0·005247		Schmidt and Wenner

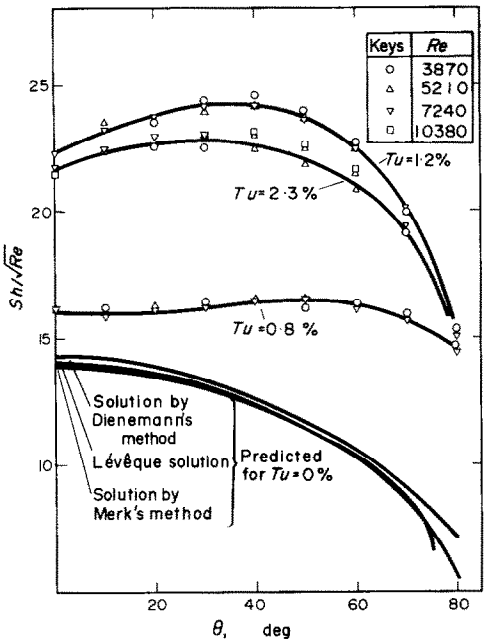

FIG. 7. Variation of local mass-transfer coefficient around a cylinder with turbulence intensity, angular coordinate and Reynolds number.

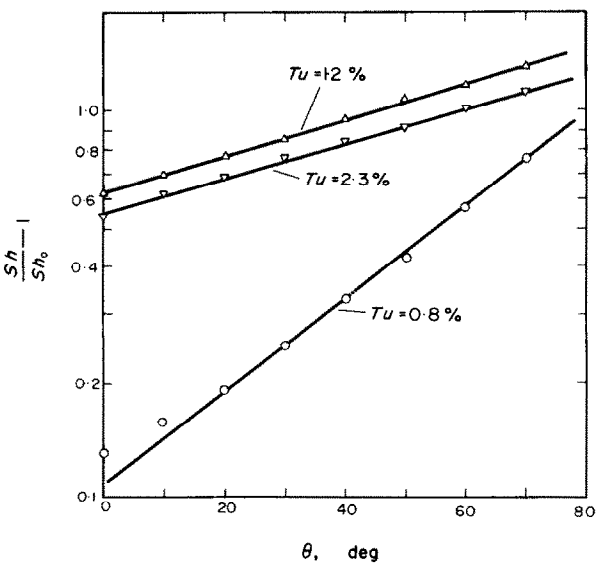

FIG. 8. Effect of turbulence on the local mass-transfer coefficient in cross flow.

previous section are plotted as the values at zero turbulence intensity. For a given Schmidt number, $Sh/\sqrt{Re}$ is a unique function of the angular coordinate if the pressure distribution is not influenced by Reynolds number. As seen in Fig. 7, the three results agree very well with each other except in the region near the separation point. In Table 2, the rates of mass transfer at the stagnation point predicted by these approximate methods are compared with the exact solution given by equations (12) and (13). This table shows that all of these approximate methods lead to satisfactory results for a Schmidt number of 1230.

(4) *Measurements of local mass-transfer coefficient.* The measurements of the local mass transfer rate around the cylinder were carried out at the three turbulence levels of 0·8, 1·2 and 2·3 per cent. The measurements were made at two symmetrical positions, denoted by $+\theta$ and $-\theta$ respectively. The discrepancy of both measured values is very small, that is, 2 per cent at most. In the following, the discussion of the effect of turbulence on the local mass transfer rate will be limited to the laminar boundary-layer region, where the predictions of mass-transfer rate at zero turbulence intensity exist.

In Fig. 7, the experimental results are plotted in the form of $Sh/\sqrt{Re}$, to be compared with the distribution at zero turbulence intensity. As seen in Fig. 7, the distributions of the local mass-transfer coefficient are represented by a family of curves, with the intensity of turbulence as a parameter. The diagram demonstrates the effect of turbulence intensity on the local mass-transfer rate, and hence on the characteristics of the

Table 2. Predicted values of mass transfer at the front stagnation point

	$Sh/\sqrt{Re}$	Error (%)
Exact solution	13·88	
Solution by Dienemann's method	14·35	+3·4
Solution by Merk's method	13·93	+0·4
Lévêque's solution	14·11	+1·7

laminar boundary layer. Moreover, this figure shows that at the front stagnation point, there is a minimum in measured local mass-transfer rate, in contrast with the prediction for zero turbulence intensity. Grassmann [6] also detected this phenomena, and measured the fluctuation of local mass-transfer rate near the stagnation point. His results show that the fluctuation of mass-transfer rate is negligible at the stagnation point, and that it increases and then decreases again as the angle θ is increased. Such a behaviour of fluctuation corresponds to the distribution of mass transfer coefficients near the stagnation point.

From the curves in Fig. 7, the ratio of the difference between the measured Sherwood number and that for zero turbulence intensity to the latter, i.e. $(Sh - Sh_0)/Sh_0$ are calculated and plotted against θ on a semi-log scale in Fig. 8. Different straight lines are obtained for each turbulence intensity. With increase of the angle θ, this ratio increases, i.e. the effect of

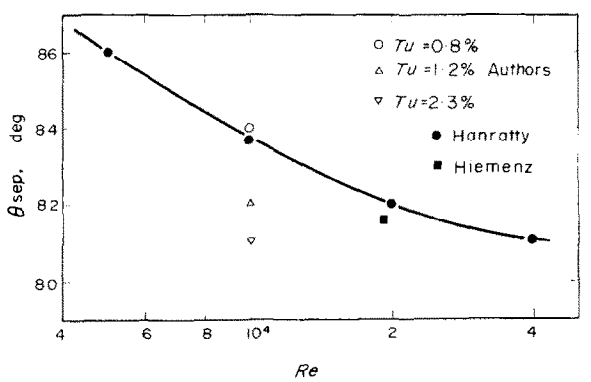

FIG. 9. Variation of the location of the separation point with turbulence intensity and Reynolds number.

turbulence increases. Figure 8 indicates that the effect of turbulence on the local mass-transfer rate may be expressed as follows:

$$\frac{Sh}{Sh_0} - 1 = f(Tu)\exp\left[g(Tu)\,\theta\right]. \qquad (17)$$

Since the effect of the turbulence intensity becomes very large near the separation point, it is expected that the turbulence intensity influences the separation of the boundary layer. Since large vortexes are shed at the separation point, the fluctuation of the local mass-transfer rate reaches a sharp maximum there, so that the separation point is determined by measuring the fluctuation. The separation point at $Re = 10000$ was determined by this method to be $\theta_{sep} = 81°$, 82° and 84° at turbulence intensity of 2·3, 1·2 and 0·8 per cent respectively. The angles of separation are presented in Fig. 9 together with those measured in low-turbulence wind tunnels by other investigators [17]. It is seen that the angle of separation at the smallest turbulence intensity, 0·8 per cent, is in good agreement with the results by other investigators and that the angles of separation become smaller with increasing turbulence intensity. These angles are smaller than the predicted value $\theta_{sep} = 85{\cdot}2°$ from the Blasius series. It may be concluded that the increase in the turbulence intensity of the free stream promotes noticeable movement of the separation point in the upstream direction.

CONCLUDING REMARKS

1. An analogy exists between the overall mass transfer for high Schmidt number and the overall heat transfer for $Pr = 0{\cdot}7$. Even in the effect of turbulence on the overall transfer rates, an analogy persists. At low turbulence intensities, a slight increase in intensity causes substantial increases in the mass-transfer rate, but the transfer rate becomes almost constant at high turbulence intensities.

2. The effect of turbulence on the local mass-transfer rate becomes larger with the increase in the angle from the front stagnation point.

3. The increase in turbulence intensity in the free stream promotes noticeable movement of the stagnation point in the upstream direction.

The present study demonstrates clearly the effects of free-stream turbulence on mass-transfer rate. However, it is not sufficient for the theoretical analysis of this phenomena.

Further investigations of the detailed mechanism of changing velocity and concentration fluctuations in the laminar boundary layer by free-stream turbulence are required. For this purpose, the electrochemical method seems to be very useful in the measurement of the fluctuation of local shear stress and mass-transfer rate.

REFERENCES

1. E. W. COMINGS, J. T. CLAPP and J. F. TAYLOR, Air turbulence and transfer process—Flow normal to cylinders, *Ind. Engng Chem.* **40**, 1076 (1948).
2. W. H. GIEDT, Effect of turbulence level of incident air stream on local heat transfer and skin friction on a cylinder, *J. Aero. Sci.* **18**, 726 (1951).
3. J. KESTIN and P. F. MAEDER, Influence of turbulence on the transfer of heat from cylinder, NACA TN 4018 (1957).
4. T. MIZUSHINA, Electrochemical method in transport phenomena, *Advances in Heat Transfer*, Vol. 7. Academic Press, New York, London (1970).
5. A. POPE, *Wind Tunnel Testing*, 2nd ed. John Wiley, New York (1954).
6. P. GRASSMANN, N. IBL and J. TRÜB, Elektrochemische Messung von Stoffübergangszahlen, *Chemie-Ingr-Tech.* **33**, 529 (1961).
7. R. HILPERT, Wärmeabgabe von geheizten Drähten und Rohren im Luftstrom, *Forsch. Geb. Ing-Wes.* **4**, 215 (1933).
8. N. FRÖSSLING, Verdunstung, Wärmeübergang und Geschwindigkeitsverteilung bei zweidimensionaler und rotationssymmetrischer laminarer Grenzschichtströmung, Lunds Universitets Arsskrift, N. F. Avd. 2, **36**, No. 4 (1940).
9. W. DIENEMANN, Berechnung des Wärmeüberganges an laminar unströmten Körpern mit konstanter und ortsveränderlicher Wandtemperature, *Z. Angew. Math. Mech.* **33**, 89 (1953).
10. H. J. MERK, Rapid calculations for boundary-layer transfer using wedge solutions and asymptotic expansions, *J. Fluid Mech.* **5**, 460 (1959).
11. D. MEKSYN, The laminar boundary-layer equations, Part I, Motion of an elliptic and circular cylinders, *Proc. R. Soc.* **192A**, 545 (1947).
12. A. ACRIVOS, Solution of the laminar boundary layer energy equation at high Prandtl numbers, *Physics Fluids* **3**, 657 (1960).
13. S. GOLDSTEIN, *Modern Developments in Fluid Mechanics*, Vol. 2. Oxford University Press, London (1938).
14. H. SCHLICHTING, *Boundary Layer Theory*, transl. by J. KESTIN, 4th ed. McGraw-Hill, New York (1960).
15. S. GOLDSTEIN, *Modern Developments in Fluid Mechanics*, Vol. 1. Oxford University Press, London (1938).
16. H. H. SOGIN, V. S. SUBRAMANIAN and R. J. SOGIN, Heat transfer from surface of non-uniform temperature distribution, AFOSR Tech. Rep. 60 (1960).
17. J. SON and T. J. HANRATTY, Velocity gradients at the wall for flow around a cylinder at Reynolds numbers from 5×10^3 to 10^5, *J. Fluid Mech.* **35**, 353 (1969).

EFFET DE LA TURBULENCE DE L'ÉCOULEMENT LIBRE SUR LE TRANSFERT MASSIQUE POUR UN CYLINDRE CIRCULAIRE DANS UN ÉCOULEMENT FRONTAL

Résumé—On présente pour un grand domaine du nombre de Schmidt le transfert massique local et global relatif à un cylindre circulaire dans un écoulement frontal. Des mesures du transfert massique ont été faites par une méthode électrochimique à trois niveaux d'intensité de turbulence, $Tu = 0{,}8$; 1,2 et 2,3% et pour un domaine du nombre de Reynolds compris entre 3870 et 10380.

On a déterminé pour un nombre de Schmidt égal à 1230 l'effet de la turbulence produite par une grille dans l'écoulement libre sur les flux massiques locaux et globaux. De plus, on a déterminé l'effet de la turbulence sur la localisation du point de séparation.

EINFLUSS DER FREISTROMTURBULENZ AUF DEN STOFFTRANSPORT VON EINEM QUERANGESTRÖMTEN KREISZYLINDER

Zusammenfassung—Es werden der gesamte und der örtliche Stofftransport von einem querangeströmten Kreiszylinder in einem grossen Bereich der Schmidt-Zahl behandelt. Messungen des Stofftransportes wurden mit Hilfe einer elektrochemischen Methode bei drei Turbulenzgraden $Tu = 0{,}8$, 1,2 und 2,3 Prozent und im Bereich der Reynolds-Zahlen 3870 bis 10380 durchgeführt.

Der Einfluss sieberzeugter Turbulenz im Freistrom auf den gesamten und den örtlichen Stoffstrom wurde bei der hohen Schmidt-Zahl von 1230 bestimmt. Zusätzlich wurde der Einfluss der Turbulenz auf den Ort des Ablösepunktes bestimmt.

ВЛИЯНИЕ ТУРБУЛЕНТНОСТИ СВОБОДНОГО ПОТОКА НА ПЕРЕНОС МАССЫ ПРИ ПОПЕРЕЧНОМ ОБТЕКАНИИ КРУГОВОГО ЦИЛИНДРА

Аннотация—Приведены данные для общего и локального переноса массы при поперечном обтекании кругового цилиндра. Измерения массообмена проводились электрохимическим методом при трёх степенях турбулентности: $Tu = 0{,}8$; 1,2 и 2,3% и числе Рейнольдса от 3870 до 10380.

Влияние экранных турбулизаторов в свободном потоке на общую и локальную скорости массообмена определялось при числе Шмидта 1230. Кроме того, определялось влияние турбулентности на точку отрыва.